Mansoura Engineering Journal

Volume 28 | Issue 1 Article 5

1-1-2021

Hydraulic Characteristics of Submerged Flow in Non-Prismatic Stilling Basins.

A. Negm
Department of Water & Water Structures Engineering., Faculty of Engineering., Zagazig University., Zagazig, Egypt, amnegm85@hotmail.com

G. Abdel-Aal
Department of Water & Water Structures Engineering., Faculty of Engineering., Zagazig University. Zagazig., Egypt.

M. Elfiky
Department of Water & Water Structures Engineering., Faculty of Engineering, Zagazig University., Zagazig, Egypt.

Y. Mohamed
Department of Water & Water Structures Engineering., Faculty of Engineering, Zagazig University., Zagazig, Egypt.

Follow this and additional works at: https://mej.researchcommons.org/home

Recommended Citation

Negm, A.; Abdel-Aal, G.; Elfiky, M.; and Mohamed, Y. (2021) "Hydraulic Characteristics of Submerged Flow in Non-Prismatic Stilling Basins.," *Mansoura Engineering Journal*: Vol. 28 : Iss. 1 , Article 5.
Available at: https://doi.org/10.21608/bfemu.2021.140761

This Original Study is brought to you for free and open access by Mansoura Engineering Journal. It has been accepted for inclusion in Mansoura Engineering Journal by an authorized editor of Mansoura Engineering Journal. For more information, please contact mej@mans.edu.eg.

HYDRAULIC CHARACTERISTICS OF SUBMERGED FLOW IN NON-PRISMATIC STILLING BASINS

الخصائص الهيدروليكية للسريان المغمور فى أحواض التهدئة غير منتظمة الشكل

A. M. Negm[1], G. M. Abdel-Aal[1], M.M. Elfiky[1], and Y. Abdalla Mohamed[2]
[1] Associate Pfofessors and [2] Assistant Lecturer
Dept. of Water & Water Structures Eng., Faculty of Engineering,
Zagazig University. Zagazig, Egypt, E-mail: amneem85@hotmail.com

خلاصة:

يتناول البحث عرض نتائج الدراسات النظرية والمعملية التى أجريت على أحواض تهدئة غير منتظمة الشكل لكشف النقاب عن تأثير استخدام أعتاب النهاية على خصائص السريان المغمور (متمثلة فى القفزة الهيدروليكية المغمورة) في أحواض التهدئة القطرية المحتوية على انخفاض مفاجئ فى القاع. فى الدراسة المعملية، اختبر تأثير موضع انخفاض القاع داخل حوض التهدئة القطرى عند وجود عتب نهاية متغير الارتفاع. وبتحليل النتائج المعملية تبين ان تأثير وجود عتب النهاية مع انخفاض القاع ينتج تأثير على خصائص السريان يقع بين تأثير عتب النهاية منفردا وتأثير انخفاض القاع منفردا حيث يقلل العتب فقط من طول القفزة الهيدروليكية المغمورة ويزيد من إهدار الطاقة (وإن كان التأثير محدودا) ويزيد انخفاض القاع من طول القفزة ويقلل من قيمة الطاقة المهدرة مقارنة بحالة عدم احتواء حوض التهدئة علي عتب نهاية أو انخفاض فى القاع. وقد تبين من مقارنة نتائج الدراسة النظرية بتلك المعملية أن هناك توافقا جيدا مما يشجع استخدام المعادلات النظرية المشتقة (على أساس تطبيق نظرية كمية الحركة) فى الحالات الشبيهة فى الطبيعة.

ABSTRACT

Recently, the non-prismatic stilling basins attracted many researchers due to their effective dissipation of excess energy. Radial stilling basins are characterizing with symmetric flow patterns that in turn minimize the expected damages of the erodible bed downstream the stilling basins. In this research, the submerged flow in radial stilling basin was provided with negative step and an end sill was analyzed both theoretically and experimentally. The effects of various parameters such as submergence, relative height of sill, relative height of step and inlet Froude number were presented and discussed. The experimental study is conducted on 30 cm wide, 45 cm deep and 12 m long open channel. The theoretical study utilized the one-dimensional momentum and continuity equations. The developed equations are verified using the obtained experimental data. Also, prediction models to estimate the length of jump are developed using the dimensional analysis and statistical methods. The models are calibrated and verified using the experimental data.

INTRODUCTION

The presence of a negative step or a sudden drop in the bed of the channel is sometimes necessary and cannot be avoided based on the topography of the land where the channel is to be constructed. The effect of constructing sudden drops in radial stilling basins were not well investigated yet to the best knowledge of the authors. However, the effect of the drop on the flow characteristics in rectangular prismatic channels was studied in horizontal channels by Hager (1985), Hager and Singer (1985), Hager and Bretez (1986) and Ohtsu and Yasuda (1991). The B-jumps at an abrupt drop was studied (Hager, 1985). It was found that the relative energy dissipation became insignificant when F_1=8.0, and the maximum energy dissipation occur for relative drop height equal to 2.5. Also, the positive and negative steps in horizontal channel were investigated, Hager and Bretez (1986). They derived analytically the relationships between A-jump and B-jump. Moreover the transition from supercritical to subcritical flow at an abrupt drop was studied, Ohtsu and Yasuda (1991). Later on, the hydraulic jumps at positive and negative steps on sloping floors were studied by Negm (1996) and a prediction model for computing the sequent depth ratio of the hydraulic jump was developed. Recently, the effects of negative step on pressure fluctuations at the bottom of a hydraulic jump was investigated. Armenio et al (2000).

Accepted March 3, 2003.

On the other hand, different types of sills may be used to produce forced jumps. The effect of the sill on the jump characteristics depends on factors such as the sill configuration, sill location and sill spacing when more than one sill was used. Several investigations dealt with the effect of sill on the hydraulic jump characteristics when the sill was constructed beneath hydraulic jump e.g. Rajaratnam, (1967), Ohtsu et al. (1991), Hager and Li (1992) and Ezzeldin et al. (2000). Other studies on the effect of vertical sill on the jump and different classification of jumps due to presence of sill could be reviewed in Hager (1992). One of these classifications of the forced hydraulic jump due to vertical sill was given by Hager and Li (1992). They classified the jump over vertical sill into A-jump, B-jump, minimum B-jump and C-jump. The A-jump was corresponding to the classical hydraulic jump, which was characterized by the maximum sequent depth ratio for the free jumps. They stated that A-jump in which the jump characteristics were not influenced by the presence of sill (or weak effect was presented) as the sill was found at the end of the surface roller and thus it was outside the effective zone for the sill to affect the jump flow. The effect of end sill in radial stilling basins was investigated by Negm et al. (2002a). They found that, theoretically and experimentally, the sill decreased slightly the relative length of jump and increased slightly the relative energy loss.

The characteristics of the submerged jump in rectangular channels were presented and discussed by many investigators e.g. Goivanda and Rajaratnam (1963). Numerical investigations on submerged jump in rectangular channels include those of Long et al. (1991) and Ma et al. (2002). A systematic investigation on transition from supercritical to subcritical flow for submerged jump below an expanding outlet was conducted Ohtsu et al. (1999). The submerged radial jump was investigated theoretically and experimentally by McCorquodale and Khalifa (1980).

The present research aims to investigate the combined effect of both negative step and end sill on the hydraulic characteristics of radial submerged hydraulic jump.

DEVELOPMENT OF THE THEORETICAL MODELS

Figure 1 presents a definition sketch for submerged hydraulic jump in radial basin which is provided with a negative step and an end sill with sloping upstream face and vertical downstream face as recommended by USBR (1958).

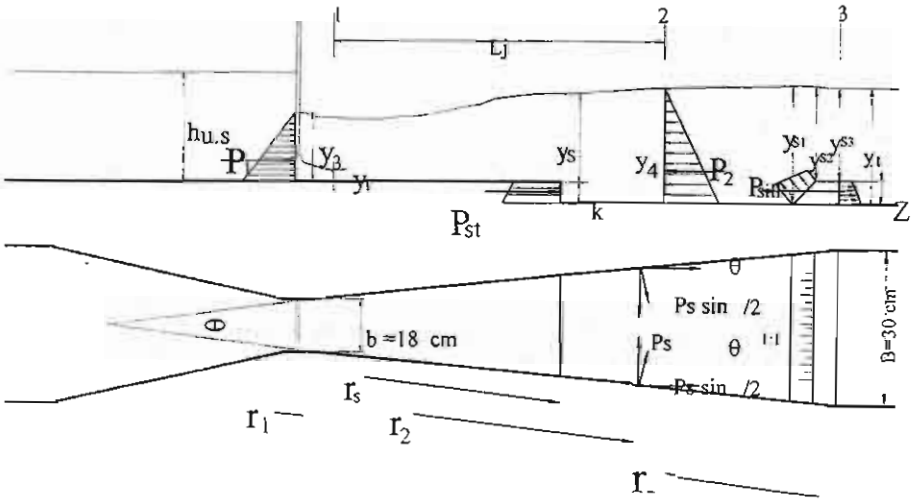

Fig. 1 Definition Sketch showing the formation of submerged hydraulic jump in radial basin containing a step and an end sill

All the variables are defined at the end of this research. Both the 1-D momentum and continuity equations are used to develop a theoretical design model for computing either the submergence ratio or the sequent depth ratio (in terms of the other one) of the submerged hydraulic jump formed in radial stilling basin provided with a negative step and an end sill. The development of the model is carried out using two control volumes, each of them takes place at the beginning of the jump, one of them ends at the end of the jump (assuming no effect of the end sill) and the second ends at the end of the basin (to evaluate the effect of sill).

The present development is based on the following assumptions: (a) the flow is radial and steady, (b) the liquid is incompressible (c) The channel is horizontal and has smooth boundaries, (d) hydrostatic pressure distribution at the beginning and at the end of the jump, (e) uniform velocity distribution at the beginning and at the end of control volumes (values of the kinetic energy correction factor and the momentum correction factor, α and β were equal to unity) and (f) the effects of air entrainment and turbulence are neglected.

The momentum equation has the form of equation (1) when applied to the control volume 1-3:

$$P_1 - P_2 + 2P_s \sin\frac{\theta}{2} + P_{st} + P_{sl} = \frac{\gamma}{g} Q(V_2 - V_1) \qquad (1)$$

In which P_1 and P_2 are the hydrostatic pressure forces at the vena contracta and at the end of the control volume respectively, P_s is the channel side pressure force, P_{st} is the pressure force acting on the step of height k at a radial distance r_s and depth of flow y_s, P_{sl} is the pressure force on the sill, V_1 and V_2 is the velocities at vena contracta and at the end of the control volume respectively, Q is the discharge, γ is the specific weight of water, g is the gravitational acceleration and θ is the angle of divergence of the radial basin. The pressure forces are given in Table 1 for both control volumes 1-2 and 1-3.

Table 1 Pressure forces and symbols at the considered control volumes 1-2 and 1-3.

Forces or Symbols	Control volume 1-2	Control volume 1-3
P_1	$\gamma r_1 y_3^2 \sin\frac{\theta}{2}$	$\gamma r_1 y_3^2 \sin\frac{\theta}{2}$
V_1	$Q/(2r_1y_3\sin(\theta/2))$	$Q/(2r_1y_3\sin(\theta/2))$
P_2	$\gamma r_1 y_4^2 \sin\frac{\theta}{2}$	$\gamma B y_t^2$
V_2	$Q/(2r_2y_4\sin(\theta/2))$	$Q/(By_t)$
P_s	$0.5\gamma\left[(r_2 - r_1)\bar{y}^2 - (r_s - r_1)k^2\right]$	$0.5\gamma\left[(r_e - r_1)\bar{y}^2 - (r_s - r_1)k^2\right]$
$\bar{y}$	$\sqrt{(y_3 + k)y_4}$	$\sqrt{(y_3 + k)y_t}$
P_{st}	$2\gamma(y_sk+0.5k^2)r_s\sin(\theta/2)$	$2\gamma(y_sk+0.5k^2)r_s\sin(\theta/2)$
P_{sl}	No sill	$\gamma Bz[y_{s3}+0.5z-0.5(y_{s1}+y_{s2})]$
V_{sl}	-	$Q/(By_{s3})$
E_1	$k + y_3 + V_1^2/2g$	$k + y_3 + V_1^2/2g$
E_2	$z + y_4 + V_2^2/2g$	$z + y_{s3} + V_{sill}^2/2g$
Y_2	y_4/y_1	y_t/y_1
r_2	r_2/r_1	r_e/r_1

Substituting from Table 1 using quantities of CV 1-3 into equation (2), then dividing by $(\gamma r_1 y_1^2 \sin\theta/2)$ and simplify to obtain:

$$S^2 + SY_o(b_o - 1) + Y_o(b_o - 1)K_o - (r-1)K_o^2 - b_o Y_o^2 + 2(Y_S K_0 + 0.5K_0^2)r + 2b_o Z_o Y_{S3} + Z_o^2 b_o - b_o Z_o(Y_{S1} + Y_{S2}) - 2F_1^2(1/(b_o Y_o) - 1) = 0 \quad (2)$$

In which, $S = \frac{y_3}{y_1}$, $b_o = \frac{b_1}{B}$, $r = \frac{r_s}{r_1}$, $K_o = \frac{k}{y_1}$, $Y_s = \frac{y_s}{y_1}$, $Z_o = \frac{z}{y_1}$, $Y_{s1} = \frac{y_{s1}}{y_1}$, $Y_{s2} = \frac{y_{s2}}{y_1}$, $Y_{s3} = \frac{y_{s3}}{y_1}$.

The solution of equation (2) leads to

$$S = -0.5A_* + \sqrt{\begin{matrix}0.25A_*^2 - K_o A_* + (r-1)K_o^2 + b_o Y_o^2 - 2(Y_S K_o - 0.5K_o^2)r \\ -2b_o Z_o Y_{S3} - b_o Z_o^2 + b_o Z_o(Y_{S1} + Y_{S2}) + 2F_1^2(1/(b_o Y_o) - 1)\end{matrix}} \quad (3)$$

In which,

$$A_* = Y_o(b_o - 1)$$

If there is no step (K_o=0), equation (3) tends to the one developed by Negm et al. (2002a) as:

$$S = -0.5A_* + \sqrt{\begin{matrix}0.25A_*^2 + r_o Y_o^2 - 2b_o Z_o Y_{S3} - b_o Z_o^2 + b_o Z_o(Y_{S1} + Y_{S2}) \\ +2F_1^2(1/(b_o Y_o) - 1)\end{matrix}} \quad (4)$$

and if there is no end sill (Z_o=0, CV 1-2) equation (3) becomes, Negm et al. (2002b):

$$S = -0.5A_* + \sqrt{\begin{matrix}0.25A_*^2 - K_o A_* + (r-1)K_o^2 + r_o Y_o^2 - 2(Y_S K_o + 0.5K_o^2)r \\ +2F_1^2(1/(r_o Y_o) - 1)\end{matrix}} \quad (5)$$

Similarly, if both K_o=0 and Z_o=0, equation (3) tends to the equation derived by McCorquodale and Khalifa (1980) in the form:

$$S = -0.5A_* + \sqrt{0.25A_*^2 + r_o Y_o^2 + 2F_1^2(1/(r_o Y_o) - 1)} \quad (6)$$

Equation (3) could be rearranged to yield a third degree polynomial in Y_o as follows:

$$b_o Y_o^3 - (S + K_o)(b_o - 1)Y_o^2 - [S^2 + 2F_1^2 + 2(Y_S K_o + 0.5K_o^2)r - (r-1)K_o^2 + 2b_o Z Y_{S3} + Z_o^2 b_o - b_o Z_o(Y_{S1} + Y_{S2})]Y_o + 2F_1(1/b_o) = 0 \quad (7)$$

Which will take the form of equations (8) and (9) for the cases of only end sill and only negative step respectively

$$b_o Y_o^3 - S(b_o - 1)Y_o^2 - [S^2 + 2F_1^2 + 2b_o Z Y_{S3} + Z_o^2 b_o - b_o Z_o(Y_{S1} + Y_{S2}]Y_o + 2F_1(1/b_o) = 0 \quad (8)$$

$$r_o Y_o^3 - (S + K_o)(r_o - 1)Y_o^2 - [S^2 + 2F_1^2 + 2(Y_S K_o + 0.5K_o^2)r - (r-1)K_o^2]Y_o + 2F_1(1/r_o) = 0 \quad (9)$$

Also, equation (6) could be put in the form

$$r_o Y_o^3 - S(r_o - 1)Y_o^2 - [S^2 + 2F_1^2]Y_o + 2F_1(1/r_o) = 0 \quad (10)$$

THE RELATIVE ENERGY LOSS

The energy loss through the hydraulic jump is obtained by applying the energy equation between section 1-3 as follows:

$$E_1 = k + y_3 + \frac{V_1^2}{2g} \tag{11}$$

$$E_2 = z + y_{s3} + \frac{V_{s3}^2}{2g} \tag{12}$$

By dividing equations (11) and (12) by y_1, and using continuity equation that leads to equation (13)

$$\frac{E_L}{E_1} = 1 - \frac{Z_o + Y_{s3} + 0.5F_1^2(1/(b_o Y_{s3})^2)}{K_o + S + 0.5F_1^2} \tag{13}$$

For K_o=0.0, equation (13) becomes, Negm et al. (2002a):

$$\frac{E_L}{E_1} = 1 - \frac{Z_o + Y_{s3} + 0.5F_1^2(1/(b_0 Y_{s3})^2)}{S + 0.5F_1^2} \tag{14}$$

For Z_o=0, equation (13) becomes, Negm et al. (2002b):

$$\frac{E_L}{E_1} = 1 - \frac{Y_o + 0.5F_1^2(1/(r_o Y_o)^2)}{K_o + S + 0.5F_1^2} \tag{15}$$

for both Z_o=0 and K_o=0, equation (13) assumes the same form due to (McCorquodale and Khalifa, 1980).

$$\frac{E_L}{E_1} = 1 - \frac{Y_o + 0.5F_1^2(1/(r_o Y_o)^2)}{S + 0.5F_1^2} \tag{16}$$

RELATIVE LENGTH OF JUMP

On the other hand, the use of the dimensional analysis indicated that the length of jump ratio (L_j/y_1) of the submerged radial hydraulic jump formed in radial basin with step is a function of the F_1, S, K_o, r and Z_o as follows

$$\frac{L_j}{y_1} = f(F_1, S, K_o, r, Z_o) \tag{17}$$

The function f is to be determined based on the experimental data.

DETAILS OF EXPERIMENTAL STUDY

The experimental work of this study is conducted using a recirculating adjustable flume of 12.0 m long, 45 cm deep and 30 cm wide. The discharges are measured by using pre-calibrated orifice meter fixed on the feeding pipeline. The tailgate at the downstream end of the flume is used to control the tail water depth of flow for each run. The radial basin is made from a clear prespex to enable visual inspection of the phenomenon being under investigation. The model length is kept constant at 130 cm and the angle of the divergence is kept constant at 5.28° with an expansion ratio of 1.67. A sill of 1:1 upstream slope and vertical downstream face is fixed at the end of the basin. A smooth block of wood is formed to fit well inside the basin model extending from upstream the gate by 5.0 cm to position where the step is desired. A fixed height of the negative step (drop) of 2.5 cm is used. Different positions of the step are tested under the same flow conditions (r_s=r_1, 1.16r_1, 1.33r_1 and 1.5r_1) downstream from the gate opening respectively. The model is fixed in the bed between the two side-

walls of the flume as shown in Fig. 1. A smooth baffle block of wood is formed to fit well inside the basin model extending one side of the model to the other side at the end of the basin to simulate the end sill. The wood is then well painted by a waterproof material (plastic) to prevent wood from changing its volume by absorbing water. For each model three heights of the sill are tested, viz: 3, 4 and 5 cm. The range of the experimental data are as follows: Q (4 lit/s - 11 lit/s), Froude numbers (2.0-7.0), submergence ratio (3.5 – 10.0), Y_o (4.0-12.0), r_o (1.4- 1.67), relative height of step K_o (0.0-3.5) and relative height of the sill, Z_o (0.0 to 3.5).

Each model is tested using five different gate openings with five discharges for each gate opening. The measurements are recorded for several submergence ratios for each discharge. The total numbers of runs were 430 in the presence of an end sill and 239 runs without end sill. A typical test procedure consisted of the following steps:(a) a gate opening is fixed and a selected discharge is allowed to pass. (b) the tailgate is adjusted until a submerged jump is formed. (c) once the stability conditions are attained, the flow rate, length of the jump, water depths upstream and just downstream of the gate in addition to the tail water depth and the depth of water above the step are recorded. The length of jump is taken to be the section at which the flow depth becomes almost horizontal (d) the position of the tailgate is changed to obtain another submergence ratio and then step (c) is repeated. (e) step (d) is repeated several times then the procedure is repeated for another discharge till the required discharges are covered (f) the whole procedure is repeated for another gate opening and so on till the range of the experimental data were covered.

ANALYSIS AND DISCUSSION OF RESULTS

WATER SURFACE PROFILES

A typical dimensionless water surface profile for the hydraulic jump (HJ) in radial basin (RB) with a negative step (NS) positioned at r=1.33 and an end sill (ES) of relative height Z_o=2.92 at particular initial Froude number of F_1 = 3.05 and submergence ratio of S = 6.62 is presented in Figure 2. It is also shown in the figure the profiles for smooth bed (Z_o=0.0, K_o=0.0), step only (r=1.33), and end sill only (Z_o=1.71).

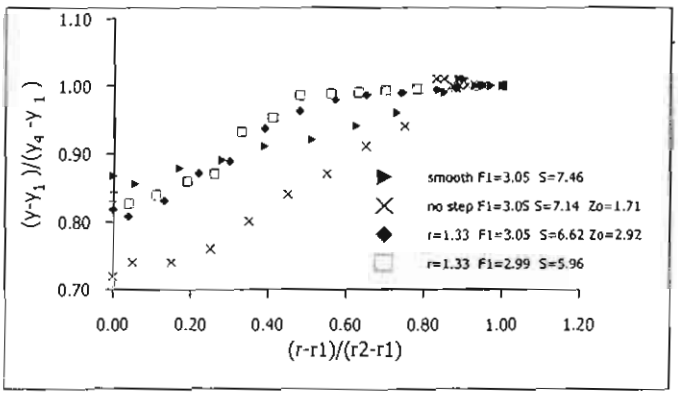

Fig. 2 Experimental dimensionless water surface profiles for submerged radial hydraulic jump at F_1=3.05

All profiles show similar trend of variation of the dimensionless depth with the dimensionless longitudinal distance. The high water surface just downstream the gate which is decreased rapidly and started to increase gradually till the water surface showed insignificant variation and became practically horizontal at the end of the HJ. The interesting observations from the shown figure are summarized as follows:

- The negative step (NS) case (r=1.33, F_1=2.99) produces higher water surface profile (WSP) if compared with (a) smooth bed case, (b) ES case, and (c) both NS and ES. The presence of an ES at F_1=3.05 and Z_o=2.92 produces lower water surface profile than that due to the effect of end sill.
- It was observed that the smooth case showed lower WSP than negative step cases that was due to the effect of negative step.
- The case of ES only showed lower WSP compared to all other presented cases (S=7.14 and Z_o=1.71 at F_1=3.05.

RELATIVE DEPTH RATIO

Two typical relationships between the experimental relative depth of the HJ (Y_o) with the initial Froude number (F_1) when the ES has an average relative heights of Z_o=1.5(1.1 - 2.0) & Z_o=2.75 (2.1 – 3.5) and the NS is located at r=1.33 for different submergence ratios, S are presented in Figures 3a and 3b. Shown also in the figures the values due to the theoretical equations, equation (9) and equation (7) for the cases when only a NS is installed in the basin and when both a NS and an ES are installed in the basin, respectively. These figures showed similar trends in both relative heights of the ES. In each case, the increased of the submergence increases the relative depth of jump remarkably when the Froude number is kept constant. Also, the depth ratio increases with the increase of the Froude number at constant submergence. Theoretically the presence of EN has little effect on the relative depth ratio of the jump with tendency of an increasing effect at lower submergence when the Froude number is relatively high (e.g. S=4 and F_1=7.0). Equation (9) which is developed based on CV 1-2 (neglecting the effect of ES) fits the data reasonably well and the deviation between equation (7) and equation (9) is small (about 1% at S=6.0 & F_1=4 as an example) and could be neglected. Similar results were concluded by Negm et al. (2002a) regarding the effect of ES on hydraulic jump formed in radial basin without step. Also, Hager and Li (1988) stated that if the sill is located near the end of the HJ in rectangular basin, it produces insignificant effect on the jump properties.

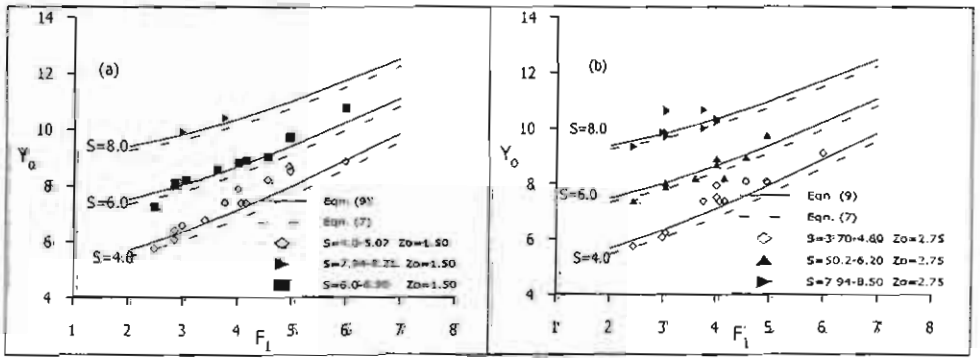

Fig. 3 Theoretical relationship between Y_o & F_1 for different S at r=1.33, (a) Z_o=1.5 and (b) Z_o=2.75.

Figure 3 shows that at the same F_1, higher submergence which could be obtained by raising the tailgate results in an increase in the depth of the HJ. At the same submergence, the relative depth of HJ increases with the increase of F_1 because higher value of F_1 means smaller y_1 (at the same Q) which yields higher Y_o (y_4/y_1) at the same S ($S=y_3/y_1$) as there is always a proportional relationship between y_4 and y_3 under submerged flow conditions.

Figure 4 presents the experimental relationship between Y_o and F_1 of HJ formed at constant S (S=5.0-5.99) to show the relative effects of no NS & no ES (smooth case), NS only, ES only and NS & ES on the same relationship. Compared to the smooth case at the same F_1, it is observed that (i) the higher the ES, the lesser the relative depth ratio due to the increase in the pressure force as the result of the presence of sill. This can be also attributed to the decrease in the specific energy above the sill compared to that upstream of the ES and since the incoming flow to the ES is subcritical, the depth of flow should be decreased.

(ii) the presence of NS increases the depth ratio of the HJ which can be explained in terms of the specific energy as follows, since the specific energy just upstream the NS is larger than that just downstream the NS and the incoming flow to the step is subcritical, the depth of flow and hence the relative depth of jump increases.

(iii) the presence of ES, when a NS exists, produces lower depth ratio compared to the case of NS only and the rate of decrease in the depth ratio increases with the increase of the relative height of the ES but still the depth ratio is more than the smooth case. This effect is mainly due to the combined effects of NS (increasing effect) and ES (decreasing effect) as explained in (i) and (ii) for each one separately.

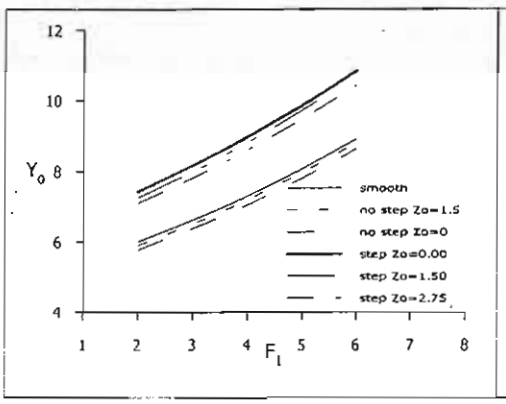

Fig. 5 Experimental relationship between Y_0 & F_1 for different r at S=3.5-3.99 and Z_0=2.75.

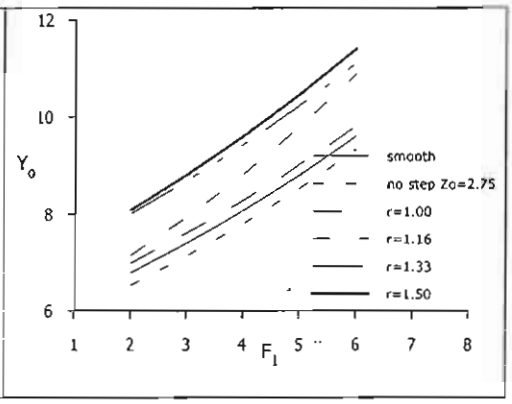

Fig. 4 Experimental relationship between Y_0 & F_1 for different Z_0 at r=1.33 and S=5.0-5.99

Figure 5 presents the experimental relationship between Y_0 and F_1 at S=6.0-6.99 and Z_0=2.75 for cases where the NS is installed at different positions. Shown also, the case of ES only and that of smooth bed (no NS & no ES). This figure confirms that the obtained observations in Fig. 4 which still valid for different positions of NS rather than the indicated one in the Figure 5. Moreover, the figure shows a systematic increase in Y_0 at constant F_1 as the NS becomes nearer to the end of the jump.

Near to the end of the jump, the impact of NS on the energy loss became small and hence a small amount of energy was dissipated. The concluded results is a lower specific energy downstream of the NS compared to that upstream of the NS and hence yielding higher depth of water leading to higher depth ratio. The rate of energy dissipation increased as the NS is moved upstream from the end of the jump yielding a smaller depth ratio because the net specific energy is smaller (e.g. specific energy at r=1.16 < specific energy at r=1.5 at the same S, F_1 and Z_0).

RELATIVE ENERGY LOSS

Figures 6a and 6b present the relationship between E_L/E_1 and F_1 for different submergence ratios at r=1.33 and average values of relative height of sill Z_0=1.5 and Z_0=2.75 respectively. It is also shown in the figures the values due to the derived equation (13) and equation (15) based on CV 1-2 and CV 1-3 respectively. The relationship between E_L/E_1 and F_1 shows the same trend of variation for both values of Z_0. At particular F_1, the E_L/E_1 increases with the decrease of submergence. This is attributed to the smaller volume of water contained in the basin at low submergence which gives more chance for roller, eddies and turbulence to develop resulting in more energy dissipation. When the submergence was kept constant, the rate of energy dissipation increases with the increase of F_1 due to created strong turbulence and eddies compared to those created at smaller F_1. On the other hand, the theoretical results based on CV 1-2 and CV 1-3 showed insignificant variation (within 1% at F_1=4.0, S =6.0) indicating that equation (15) neglected the effect of ES and accounted only the effect of NS could be used to predict reasonable values for E_L/E_1 for the HJ formed in radial basin contained a NS and an ES.

Figure 7 shows the effect of relative height of sill on the relationship between E_L/E_1 and F_1 for a typical value of S = 5.50 (S= 5.0-5.99). The ES produced higher energy dissipation with a higher rate for high ES followed by the smooth bed then the case of NS combined with ES and the lowest energy dissipation is due to the case of NS only. The presence of ES forces the jump to form within the basin and hence most of the roller and turbulence are created within the basin yielding higher energy dissipation.

The effects of step position on the relationship between E_L/E_1 and F_1 could be depicted from Fig. 8 for average value of Z_o= 2.75 (S=5.0-5.99). It is observed that moving the NS towards the end of basin caused a decrease in the energy loss and vice versa. This is because the NS near to the end of the basin produced higher water depth leading to a reduction in the formed eddies and turbulence and hence small amount of energy is dissipated. Also, it is shown in the figure, the case of only ES that produces the highest loss of energy followed by the smooth case.

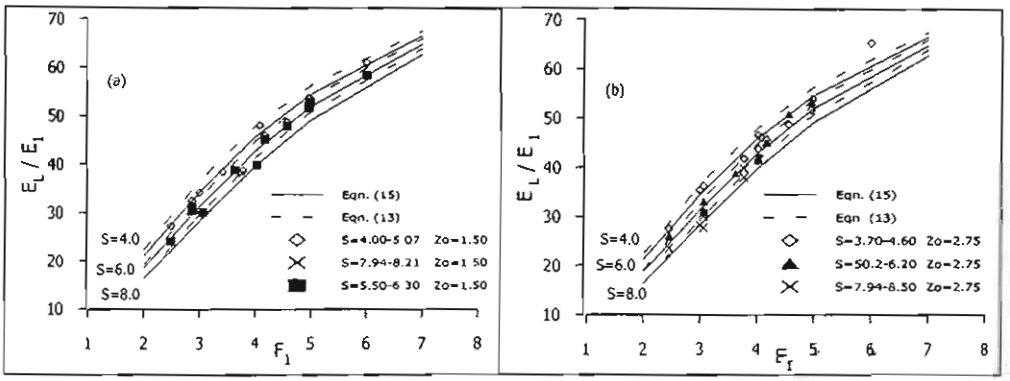

Fig. 6 Theoretical relationship between E_L/E_1 & F_1 for different S at r=1.33, (a) Z_o=1.5 and (b) Z_o=2.75.

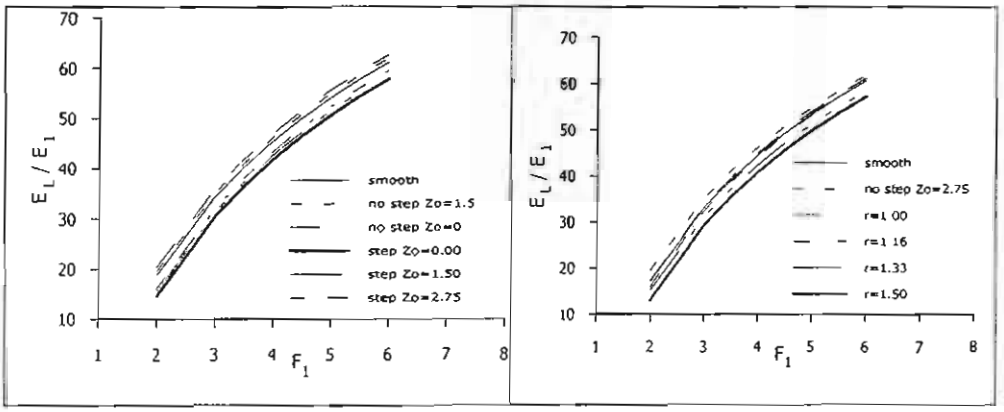

Fig. 7 Experimental relationship between E_L/E_1 & F_1 for different Z_o at r=1.33 and S=5.0-5.99.

Fig. 8 Experimental relationship between E_L/E_1 & F_1 for different step positions and Z_o=2.75 at S=6.0-6.5.

RELATIVE LENGTH OF JUMP

The relationship between Lj/y_1 and F_1 for different submergence ratios at r=1.33 is presented in Fig. 9 for Z_o=1.5. For a particular values of F_1, the increase of submergence produces a corresponding increase in the length of the jump ratio and vice versa; as more eddies and turbulence are formed at low submergence leading to shorter length of jump. Also, at small submergence, the supercritical jet of flow spreads quickly. Figure 10 presents the experimental relationship between Lj/y_1 and F_1 of HJ formed at constant S (S=5.0-5.99) to show the relative effects of smooth case, NS only, ES only and both NS and ES on the same relationship. Compared to the smooth case at the same

F_1, it is observed that, the presence of ES when a NS exists, produces lower values of Lj/y_1 compared to the case of NS only and the rate of decrease in the Lj/y_1 is increased with the increase of the relative height of the ES but the relative length of jump is still more than the smooth case (no end sill and no negative step).

Figure 11 presents the relationship between Lj/y_1 and F_1 for different relative positions of the NS at Z_o=1.5 and Z_o=2.75. These figures indicate that if the NS is installed near to the end of the basin, it produces longer length of jump and vice versa.

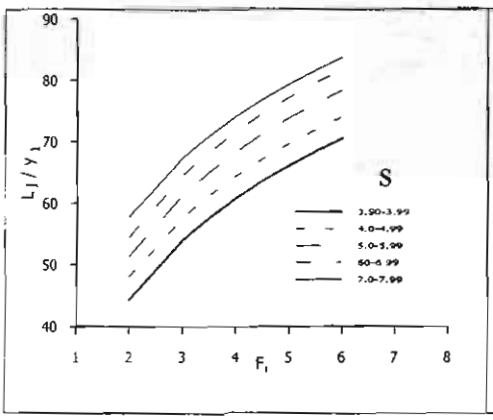

Fig. 9 Experimental relationship between Lj/y_1 & F_1 for different S at r=1.33 and Z_o=1.50.

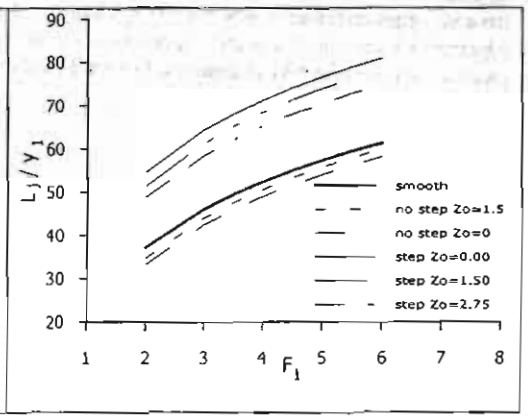

Fig. 10 Experimental relationship between Lj/y_1 & F_1 for different Z_o at r=1.33 and S=5.0-5.99.

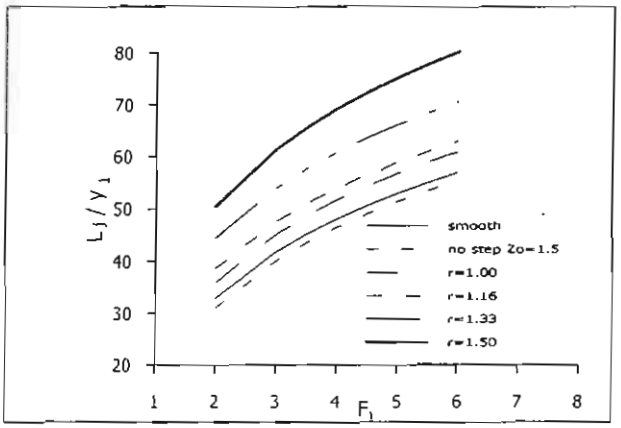

Fig. 11 Experimental Relationship between Lj/y_1 & F_1 for different step positions and Z_o=1.50 at S=3.5-3.99.

The prediction of the length of the submerged jump is possible by employing the collected data to develop empirical equations using statistical methods. Several models were tried, the following one is found to fit the data reasonably well.

$$Ln\left(\frac{L_j}{y_1}\right) = c_o + c_1F_1 + c_2S + c_3r + c_4Z_o + c_5K_o \qquad (18)$$

in which c_o, c_1, c_2, c_3, c_4 and c_5 are the regression coefficients. These coefficients were estimated using the method of least squares based on the data of NS only (239 observations) and those of NS & ES

(430 observations). The Neural Connection software (1998) was used estimate the coefficients of equation (18). Table 2 showed the values of these coefficients using all data (669 observations) for the two cases, (i) considering the effect of the ES and (ii) neglecting the effect of ES.

Table 2. Coefficients of equation (18)

Case	C_o	C_1	C_2	C_3	C_4	C_5	R^2	SEE	No. of observations.
(i)	2.766	0.083	0.061	0.510	-0.010	0.056	0.74	4.70	669
(ii)	2.760	0.080	0.061	0.525	-	0.031	0.72	4.50	669

Comparison of equation (18) with an independent set of the measured data (test data set selected randomly) is shown in Fig. 12 for both cases (i) and (ii). The prediction of equation (18) showed fair agreement in both cases. Also, Fig. 13 shows the comparison between the experimental relationship (Lj/y_1 versus F_1) and the empirical one for different submergence at r=1.33 and Z_o=1.5 (1.3-1.9). Neglecting the effect of Z_o in equation (18) yields little deviation compared to the case when the effect of Z_o is considered. This means that either equation (i) or (ii) could be used to predict the length of jump in radial basin provided with NS only or NS and ES in comparison with the existence of Z_o.

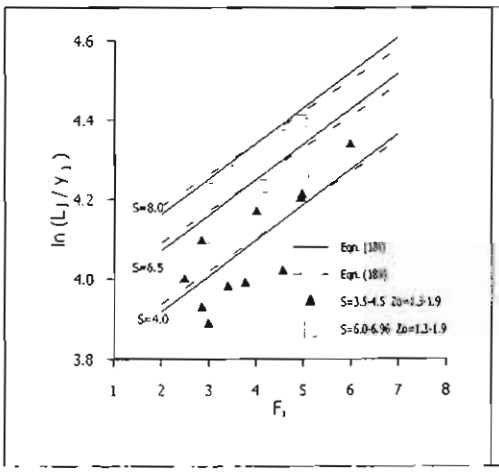

Fig. 12 Measured Lj/y_1 versus the predicted values for test data set and different step positions.

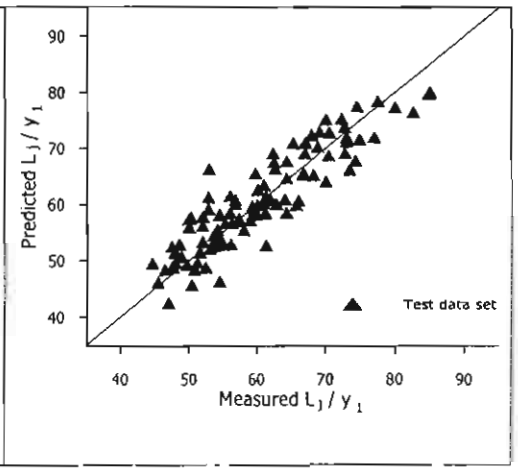

Fig. 13 Relationship between $\ln(Lj/y_1)$ & F_1 for different S according to equation (18)

CONCLUSIONS

An experimental investigation was conducted to study the effect of submergence, the relative position of negative step and the relative height of end sill on the hydraulic characteristics of the submerged hydraulic jump in radial basin. Both the relative depth and the relative length of jump decrease with the increase of the relative height of end sill while the energy loss ratio increases. However, the effect of end sill on the submerged radial jump was small for end sills of limited heights up to Z_o=3.5. Installing a negative step near to the end of the basin produces higher relative depth and longer relative length of jump compared to the negative step when it is positioned near to the beginning of the jump (near the gate). The energy loss decreases for negative step near to the end of the basin and increased when the step is constructed near the beginning of the jump. Using an end sill in a radial basin provided with a negative step causes a slight reduction on both depth and length ratios while a slight increasing effect on the relative energy loss is observed.

A theoretical equation was developed to evaluate the effect of end sill when combined with a negative step. Theoretically and experimentally, it was found that the effect of end sill has little effect on the depth and on the energy loss ratios and the theoretical equation developed for the cases of

negative steps without end sill could be used to represent also the case of negative step and end sill for limited relative height of end sill up to Z_o=3.5. For higher values of Z_o, the effect of the end sill should be considered in computing all the characteristics of the hydraulic jump in radial basins under submerged flow conditions.

REFERENCES

1. Armenio, V. Toscand, P. and Fiorotto, V. (2000), "The effects of a negative step in pressure fluctuations at the bottom of a hydraulic jump", Journal of Hydraulic Research, IAHR, Vol.38, No. 5, pp.359-368.
2. Ezzeldin, M.M. Negm, A.M. and Attia, M.I. (2000), "Forced Hydraulic jump at vertical sill Characteristics of minimum B-jump", Engineering Research Journal, Faculty of Engineering, Helwan University, Mataria, Cairo, Egypt, Vol.70, August, pp.1-21.
3. Govinda Rao, N.S. and Rajaratnam, N. (1963), "The submerged hydraulic jump", Journal of Hydraulic Div., Vol.89, No. HY1, pp.139-162.
4. Hager, W. H. (1985), "B-Jumps at Abrupt Channel Drops." Journal of Hydraulic Eng., Vol.111, No.5, pp. 861-866.
5. Hager, W.H. and Singer, R. (1985), "Flow characteristics of the hydraulic jump in a stilling basin with an abrupt bottom rise", Journal of Hydraulic Research, IAHR,Vol.23, No.2, pp 861-866.
6. Hager, W.H. and Bretz, N.V. (1986), "Hydraulic jumps at positive and negative step", Journal of Hydraulic Research, Vol. 24, No. 4, pp. 237-253.
7. Hager, W.H. (1992), "Energy dissipators and hydraulic jumps", Kluwer Academic Publications, Dordrecht, The Netherlands.
8. Hager, W.H. and Li, D. (1992), "Sill-controlled energy dissipator. Journal of Hydraulic Research, Vol. 30, No. 2, pp. 165- 181.
9. Long, D. Steffler, P.M. and Rajaratnam, N. (1991), "A numerical study of flow structure in submerged jumps", Journal of Hydraulic Research, IAHR, Vol. 29, No. 3, pp. 293-307.
10. MA, F. Hou, Y. and Perinos, P. (2002), "Numerical calculation of submerged hydraulic jumps", Journal of Hydraulic Research, IAHR, Vol. 39, No. 5, pp. 493-503.
11. McCorquodale, J.A. and Khalifa, A.M. (1980), "Submerged radial hydraulic jump", Journal of the Hydraulic Div., ASCE, Vol. 106, No. HY3, pp. 355-367.
12. Negm, A.M. (1996), "Hydraulic jumps at positive and negative steps on sloping floors", Journal of Hydraulic Research, IAHR, Vol. 34, No. 3, pp. 409-420.
13. Negm, A.M. Abdel-Aal, G. M., Elfiky, M.M. and Mohamed, Y.A. (2002a), "Theoretical and experimental evaluation of the effect of end sill on characteristics of submerged radial hydraulic jump", Scientific Bulletin, Faculty of Engineering, Ain Sham University. Cairo. Egypt, (Accepted).
14. Negm, A.M., Abdel-Aal, G. M., Elfiky, M.M., and Mohamed, Y.A. (2002b), "Submerged hydraulic jump in radial stilling basins with bottom vertical drop", Alexandria Engineering Journal, Faculty of Engineering, Alexandria University, Cairo, Egypt, (Accepted).
15. Neural Connection (1998), "ANN software and users manual", SPSS/Recognition Systems Limited.
16. Ohtsu, I. and Yasuda, Y. (1991), "Transition from supercritical to subcritical flow at an abrupt drop", Journal of Hydraulic Research, IAHR, Vol. 29, No. 3, pp.309-327.
17. Ohtsu, I. Yasuda, Y. and Ishkikawa, M. (1999), "Submerged hydraulic jump below abrupt expansions", Journal of Hydraulic Engineering, Vol. 125, No. 5, pp.492-499.
18. Ohtsu, I. Yasuda, Y. and Yamanaka, Y. (1991), "Drag on Vertical Sill of Forced Jump", Journal of Hydraulic Research, IAHR, Vol. 29, No. 1, 1991, pp.29-47, Discussions 1992, Vol. 30. No.2, pp. 277-288.
19. Rajaratnam. N. (1967). "Hydraulic jumps", in Advances in Hydro-science. (V.T. Chow editor). Vol. 4. Academic Press. New York, 1967. pp.197-280.

20. U.S. Bureau of Reclamation, (1958). "Hydraulic Design of Stilling Basins and Energy Dissipators." Engineering Monograph No. 25, Denver, Colorado.

NOTATION

The following symbols are used in this research:

B	width of the channel;
b_1	contracted width of the channel ;
E_1	total energy at the jump toe;
E_2	total energy at the jump heel;
E_L	relative energy loss;
F_1	Froude's number at the initial depth;
G	gate opening;
k	height of negative of step;
K_o	relative height of step (k/y_1);
L_j	length of the hydraulic jump;
P_1	hydrostatic pressure at the beginning of the jump;
P_2	the hydrostatic pressure at the end of the jump;
P_s	pressure force on side of the channel;
P_{s1}	pressure force due to the end sill;
P_{st}	pressure force due to the negative step;
Q	discharge;
r	the relative position step r_s/r_1;
r_1	radius at the beginning of the jump ;
r_2	radius at the end of the jump;
R^2	coefficient of determination of the regression equation;
r_e	the radius at end of the basin;
r_o	radii of jump ratio (r_2/r_1);
r_s	radius at the end of the negative step;
S	submergence ratio (y_3/y_1);
V_1	average velocity at the initial depth;
V_2	average velocity at the sequent depth;
Y_0	relative tail water depth (y_4/y_1);
y_1	initial water depth;
y_3	backed-up water depth just downstream the gate ;
y_4	water depth at the end of the jump;
y_s	water depth above the end of step;
y_t	water depth at the end of the basin;
Y_s	relative water depth at negative step (y_s/y_1);
y_{s1}, y_{s2}, y_{s3}	water depths above the end sill according to Figure 1;
Y_{s1}	relative depth over the sill where the depth is y_{s1} (y_{s1}/y_1);
Y_{s2}	relative depth over the sill where the depth is y_{s2} (y_{s2}/y_1);
Y_{s3}	relative depth over the sill where the depth is y_{s3} (y_{s3}/y_1);
$\bar{y}$	the geometric mean for water surface profile according to Table 1;
z	height of end sill;
Z_o	relative height of end sill (z/y_1);
γ	specific weight; and
θ	the angle of divergence.

CHARACTERISTICS OF SEEPAGE UNDERNEATH A HEADING-UP STRUCTURE AND A SUBSIDIARY ONE

خصائص التسرب تحت منشأ حجز و آخر مساعد

By

Adel A. El-Masry Mohamed G. Abd-Alla
Irrigation and Hydraulics Department, Faculty of Engineering,
El-Mansoura University, Egypt.

خلاصة:
أحيانا يكون من الضرورى وجود منشأ مساعد خلف منشأ حجز رئيسى يكون الغرض من إنشائه تخفيف الضاغط الهيدروليكى على المنشأ الأساسى. فى هذا البحث تم دراسة الخصائص الهيدروليكية للتسرب اسفل المنشأين فى حالة حجز المياه أمامهما مع جفاف القناة فى الخلف. تمت الدراسة باستخدام نظرية العناصر المحيطة (العنصر الخطى). تم دراسة تأثير كلا من: طول الجزء المنفذ بين المنشأ الرئيسى والمساعد وكذا سمك الطبقة المسامية أسفل المنشآت. تناولت الدراسة تحديد قوة التعويم أسفل المنشآت والتصرف و الميل الهيدروليكى للمسافة بين المنشأين وخلف المنشأ المساعد وتمثيل خطوط تساوى الضغط. تم تمثيل النتائج على صورة منحنيات لا بعدية.

ABSTRACT

Sometimes. it is necessary to build a subsidiary weir downstream the heading-up structures to relief the acting head. In the present study. water prevented between the main and subsidiary structures was considered. The boundary element technique using linear elements was used to analyze the uplift pressure underneath a simple flat floor of the heading-up structure and the subsidiary weir. Seepage flow and the exit gradients were also considered. Seven cases of the distance between the heading-up structure and the subsidiary one had been considered with five thickness of the permeable layer under the structure. Obtained results were illustrated and diseussed.

INTRODUCTION

A subsidiary weir is built downstream heading-up structures to relief the acting head during the various cases of operation. In this study, the water was prevented upstream the main structure during high water levels period while the water upstream the subsidiary one was on the crest level and its downstream was dry. Many analytical and experimental studies had been carried out to evaluate the uplift pressure distribution and exit gradients for different boundary conditions and floor configurations, Harr [9]. Chawla [4] and Gray and Chawla [8] presented analytical solutions using conformal mapping technique for a floor founded on a permeable soil of infinite and finite depths, respectively, provided with finite pervious inlet and outlet surfaces and a cut-off at any general position along the

Accepted March 15, 2003.

floor. The analysis however did not cover the case of very narrow permeable portions, which considered in this study with the presence of another structure such as a subsidiary weir, Fig. 1.

El-Masry [5,6] studied the characteristics of seepage underneath a heading-up structure with insufficient pervious length downstream the structure due to the presence of lining extended to the end of the canal. El-Masry and Abd-Allah [7] studied the same present problem for different conditions. They investigated the case of just after construction, which mean maximum water level upstream the main heading-up structure and no water up and downstream the subsidiary one.

The main objective of the study is, to study the development of uplift pressure, exit gradient and seepage flow, which affect the stability of heading-up structure and subsidiary one. Influence of changing the distance of the pervious length between the structures (S) and the permeable soil thickness beneath the floors (T) to be studied. The target is to develop the curves that express the relationships between the variables involved in this study.

In the present study, the Boundary Element Method (BEM) as a numerical technique was used to analyze the practical problem of seepage under simple flat floors of heading-up structure and the subsidiary one. The ratio between the up-stream head on the subsidiary structure (H_2) and the head on the main one (H_1) was considered to be constant and expressed as 0.4 (H_2=0.4H_1). The middle surface length between floors (S) varied from half to double the head (H_1) with an interval of 0.25. Different permeable layer thickness under the floor (T) was considered as: 0.80, 1.00, 1.20, 1.50 and 2.00 of the head (H_1). To define the considered domain (D), the inlet surface length (L) was assumed equal to the length of the first floor (L_1); end surface length (Z) was assumed 1.5 L_1. Length of subsidiary floor (L_2) was assumed to be half the length L_1. Soil beneath the structures was assumed to be homogeneous and isotropic with permeability coefficient (K). Herein, variables were allocated along the middle surface length (S) besides the thickness of soil layer (T), while other parameters were kept constant. Inflow upstream the main structure (Q_{i1}), inflow upstream the subsidiary structure (Q_{i2}), middle surface outflow (Q_{o1}) and end surface outflow (Q_{o2}) were computed and illustrated, Q is the flow per unit length.

MATHEMATICAL IDEALIZATION OF THE PROBLEM

A typical two-dimensional problem of flow through the fully saturated porous media is shown in Fig. 2. Using principles of continuity of incompressible flow and Darcy's law, the governing equation of seepage in a two-dimensional flow domain (**D**) can be described by Laplace equation (1).

$$\frac{\partial^2 h}{\partial x^2} + \frac{\partial^2 h}{\partial y^2} = 0 \qquad \text{, in } D \tag{1}$$

in which:

$h = (p/\gamma + y)$ is the potential head, and

p/γ : is the pressure head, while y: is the elevation head.

For a confined domain of seepage flow, there are two types of boundaries:

1. A prescribed head on the upstream and downstream permeable surfaces (A-B, C-D and E-F),
2. A prescribed flux on boundaries (B-C, D-E, F-G, G-J and J-A).

The boundary conditions on A-B, C-D and E-F can be described by the following set of equations:

$h = H_1$ on **A-B** (2-a)

$h = H_2$ on **C-D** (2-b)

$h = 0$ on **E-F** (D.S. is dry) (2-c)

The boundary conditions for the impervious boundaries can be described as:

$$\frac{\partial h}{\partial n} = 0 \tag{3}$$

Where

$\partial h/\partial n$ is the hydraulic gradient in the direction perpendicular to the boundary surface.

BOUNDARY ELEMENT FORMULATION

In the boundary element method, the boundary of a flow region was divided into several linear segments connected by nodal points as shown in Fig. 2. The heads and the gradients on the boundary nodes were denoted as $\{h\}$ and $\{\partial h/\partial n\}$,

respectively. The value of head or gradient at any point on a line segment between two nodes could be obtained by using interpolation functions ⟨N⟩ and {M} , Paris and Canas[12], as follows:

$$h = \langle N \rangle \{h\} \tag{4}$$

$$\frac{\partial h}{\partial n} = \langle M \rangle \left\{ \frac{\partial h}{\partial n} \right\} \tag{5}$$

where

⟨ ⟩ and { } represent a row vector and a column vector, respectively. In this presentation, ⟨N⟩ is chosen to be as ⟨M⟩, both being linear functions using Green's theorem, the volume integral of the Laplace equation can be reduced to a boundary integral, Brebbia [3]:

$$\alpha(x)\, h(x) \int_{\Gamma} \left\{ G(\zeta, x) \frac{\partial h}{\partial n}(\zeta) - F(\zeta, x)\, h(\zeta) \right\} d\Gamma(\zeta) \tag{6}$$

where

h(x) is the potential at x, G (ζ, x) and F (ζ, x) represent the potential head and gradient at field point ζ due to a unit concentrated source at source point x (i.e., the fundamental solution), respectively. For two dimensional problems, Brebbia [3]:

$$G(\zeta, x) = \frac{1}{2\pi} \ln\left(\frac{1}{r}\right) \quad r = |\zeta - x| \tag{7}$$

$$F(\zeta, x) = \frac{1}{2\pi} \frac{\partial r}{\partial n} \tag{8}$$

Using the rigid-body analogy, Banerjee and Butterfield [1], the value of α can be evaluated by:

$$\alpha(x) = \begin{cases} 1 & x \text{ in } D \\ -\int F(\zeta, x)\, d\Gamma(\zeta) & x \text{ on } \Gamma \\ 0.5 & x \text{ on } \Gamma \text{ and } \Gamma \text{ is smooth} \end{cases} \tag{9}$$

Substituting the interpolation functions into eq. (6). The relationship between heads and gradients at the boundary nodal points of a given domain is given by:

$$[H]\{h\} = [G]\left\{ \frac{\partial h}{\partial n} \right\} \tag{10}$$

In the above, the matrices [H] and [G] are obtained from:

$$[H] = [\delta]\{\alpha(x^m)\} - \int\{F(x^m,\zeta)\}\langle N(\zeta)\rangle d\Gamma(\zeta) \quad (11)$$

$$[G] = \int_\Gamma \{G(x^m,\zeta)\}\langle N(\zeta)\rangle d\Gamma(\zeta) \quad (12)$$

in which:

δ : is the Kronecker delta, x^m : is the point of node m,

ζ : is the field point on the boundary surface Γ and

$\langle N(\zeta)\rangle$: is the interpolation function.

In a boundary value problem, either gradient or potential head is known for a given node on the boundary. Therefore, eq.(10) gives a set of simultaneous equations that can be solved for the unknown variables. The boundary element method which has been outlined for a homogeneous flow domain is fairly standard and can be found in the literature, [1,2,10,11].

The use of linear elements on the boundary leads to a problem at corner points, which have two values for the head h and the normal derivative $\partial h/\partial n$ depending on the side under consideration. At these points, it is essential to select which of the two variables h or $\partial h/\partial n$ will be prescribed. As $\partial h/\partial n$ can not be defined, one generally will choose to prescribe h. This however, does not produce a very accurate computed value for the derivatives at the corners. This problem does not occur in finite elements due to the way in which the natural boundary conditions are prescribed and the fact that the solution is also approximated in the domain, i.e. errors tend to be more distributed. To avoid the corner problem, it is considered that, there are two points very near to each other but belong to different sides Fig. 2. At one node, h condition is prescribed while $\partial h/\partial n$ is prescribed at the other one.

RESULTS AND DISCUSSION

In this study, thirty-five runs were computed using the boundary element method. For the considered study, the following parameters were considered:

1. Relative distance (S/H_1) varied from 0.50 to 2.0 (0.50, 0.75, 1.0, 1.25, 1.50, 1.75 and 2.00).
2. Relative thickness of the permeable layer (T/H_1) changed from 0.8 to 2.0 (0.8, 1.0, 1.2, 1.5 and 2.0).

From the obtained results, Figs. 3 & 4 were plotted to show the relationship between the relative discharge (Q/KH_1) and both of the relative thickness of the permeable layer (T/H_1) and the relative distance (S/H_1). Figure 3 shows that, increasing the relative thickness of the permeable layer increases the upstream inflow (Q_{i1}) and decreases the downstream inflow (Q_{i2}). Increasing the separate distance, S, increases the downstream inflow and decreases the upstream inflow.

From Fig.4, it is observed that, increasing the permeable layer thickness increases the downstream out flow (Q_{o2}) while the flow seeps downstream the first floor decreases. Increasing the separate distance, S, increases the out flow downstream the first floor, (Q_{o1}), while the final out flow that seeps at the rear of the downstream structure, Q_{o2}, decreases. For the considered cases, the computed error between the summation of the inflow discharge, ($Q_i = Q_{i1} + Q_{i2}$) and the total out flow ($Q_o = Q_{o1} + Q_{o2}$) is considered good as the error is not more than 0.30%.

Figure 5 shows the distribution of the computed inflow-outflow seepage discharge for two cases of $S=H_1$, $T=0.8\ H_1$, and $S=2H_1$, $T=2H_1$. From these figures, it is observed that, the separate length, S, is divided into outflow and inflow portions at point O, that point lies at about 0.55 S apart from the downstream end of the first floor.

Figure 6 shows the variation between Q/KH_1 versus S/H_1 for $T=0.8\ H_1$. In this figure, inflow-outflow curves are represented with the summation of them. From these curves, it is clear that, the summation of the inflow discharge ΣQ_i is coincided with the outflow one, ΣQ_o.

The computed uplift pressures that acting upon the main and subsidiary structures for one case of the separate distance, $S = H_1$, for all the considered thickness of the permeable layer, T/H_1, which are illustrated as shown in Fig. 7. From this figure, it is clear that, changing the relative thickness of the permeable layer has no effect on the distribution of the uplift pressure.

The influence of the relative thickness of the permeable layer on the exit gradient at the separate distance, S, is illustrated for the case of $S/H_1=2.0$ as shown in Fig. 8. From this figure, it is clear that, changing the relative thickness T/H_1, has no considerable effect. On the other hand, Fig.9 shows the illustration of the hydraulic gradient at exit (downstream the first floor) for the case of $T/H_1=2.0$. From this figure, one can observe that, increasing the distance S, increases the values of exit gradient. From these Figs. 8 & 9, it is observed that, the distribution of exit gradient curve can be divided into two portions, the first one that lies downstream the first floor, the second lies at the distance upstream the second floor. The point that divided the two portions was found to be at about 0.55 S measured from the downstream end of the first floor. These two portions represent the outflow and inflow gradients, respectively.

Hydraulic gradients at the rear exit surface downstream the second floor are represented as shown in Fig. 10. Considering the case of $T/H_1 = 2.0$, changing the relative distance $S/H_1 = 0.5$ to 2.0, the obtained hydraulic gradients are illustrated. At the second floor end, the exit gradients tend to have an infinite value.

As a result of the computed cases, equipotential lines are plotted for three cases as shown in Fig. 11.

CONCLUSIONS

Characteristics of seepage underneath a heading up structure and a subsidiary one was studied numerically using the well-known Boundary Element Method. Spacing between the structures and the permeable layer thickness were considered. Thirty-five cases were considered taking into account the above mentioned parameters.

According to the present study, it can be concluded that:

- For the cases studied, the presence of the subsidiary structure divided the outflow discharge into two parts, downstream the first floor and downstream the rear one.
- The separate distance between the heading-up structure and the subsidiary one have been divided into two portions, one belongs to the outflow discharge downstream the first floor, and the second belongs to the inflow discharge from the prevented water upstream the subsidiary structure.
- The outflow portion of the separate distance is about 0.55 its total length.
- Increasing the permeable layer thickness leads to the following:
  - increasing the inflow upstream the first floor,
  - increasing the outflow downstream the rear floor,
  - decreasing the inflow upstream the second floor, and
  - decreasing the outflow downstream the first floor.
- The separate distance between the heading-up structure and the subsidiary one had a reverse influence comparing with the thickness of the permeable layer for inflow-outflow discharge.
- The permeable layer thickness had no a considerable effect on the uplift pressure under the floor of the structures.
- The hydraulic gradient for the separate distance between the structures represents the inflow – outflow portions.
- Increasing the separate distance increases the exit gradient.
- Equipotential lines have been illustrated as a result of the present solutions.
- More future studies considering shorter and longer separate distance between the structures and the effects on seepage streams should be accomplished.

REFERENCES

1. Banerjee, P.k. and Butterfield, R., "Boundary Element Method in Engineering Science", McGraw-Hill Book Co.1981.
2. Bear, J. and Verruijt, A., "Modeling Groundwater Flow and Pollution", D. Reidal publishing Company, Dordrecht, Holland, 1987.
3. Brebbia, C. A., "The Boundary Element Method for Engineers", Pentech Press Limited, Plymouth Devon, England, 1978.
4. Chawla, A.S., "Boundary Effects on Stability of Structures", Journal of the Hydraulic Division ASCE, Vol. 98, Sept. 1971.

5. El-Masry, A.A., "Applications of the Finite Element Method to Solve Seepage Through and underneath Engineering Structures", Ph.D. thesis, Wroclaw University, Poland.
6. El-Masry, A.A., "Influence of Insufficient Pervious Length Downstream of Hydraulic Structures", Mansoura Engineering Journal (MEJ), Vol. 18, No. 2, June 1993.
7. El-Masry, A.A. and Abd-Alla, M. G., "Seepage Underneath A detached Floor of A Heading-up Structure and A Subsidiary One", Al-Azhar Engineering Sixth International Conference (AEIC), 2000, Sept. 1-4, Pp. 94-104.
8. Gary, S.P. and Chawla, A.S., "Stability of Structures on Permeable Foundation", Journal of Hydraulic Division, ASCE, Vol. 95, July 1969.
9. Harr, M.E., "Ground Water and Seepage", McGraw-Hill Book Co. Inc. New York, N.Y., 1962.
10. Liggett, J.A., "Location of Free Surface in Porous Media", J. Hydr. Div., ASCE, 103 (4), 353-365, 1977.
11. Niwo, Y., Kobayashi, S. and Fukui, T., "An Application of the Integral Equation Method to Seepage Problem", Theoretical and applied mechanics, Vol. 24, proceeding of the 24th Japan National Congress for Applied Mechanics, 479-486, 1974.
12. Paris, F. and Canas, J., "Boundary Element Method", Oxford University Press Inc. New York, 1997.

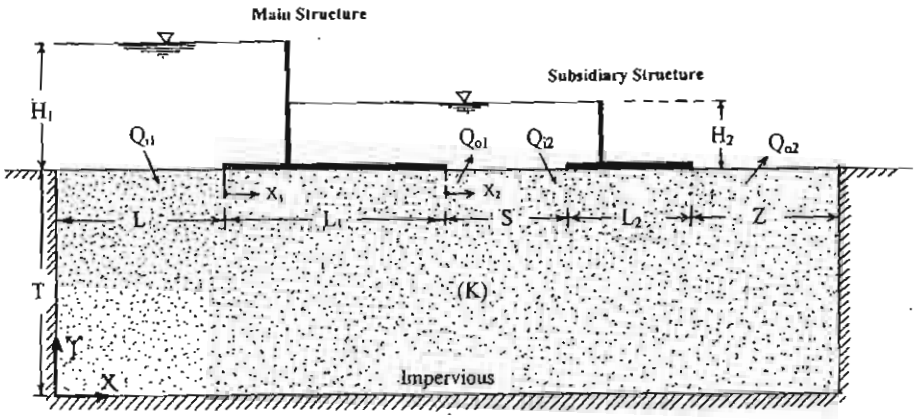

Fig. 1 Layout of the considered problem.

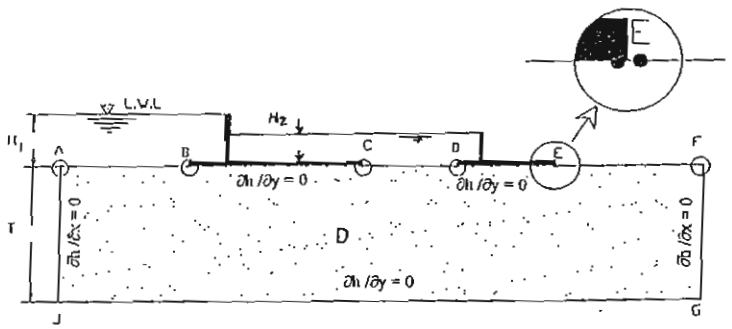

Fig. 2 Idealization of the problem.

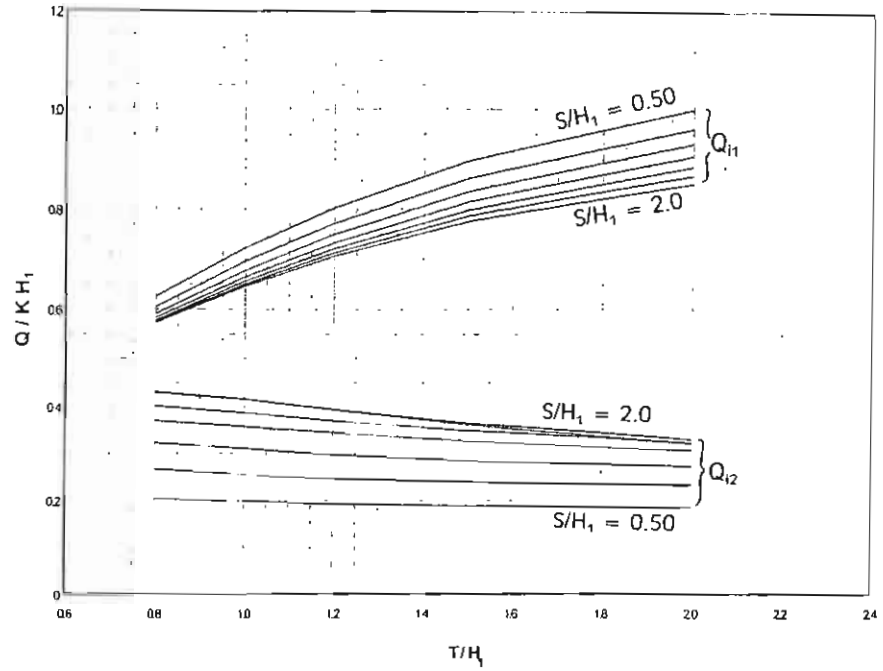

Fig. 3 Inflow upstream the first and the second floors for all S/H_1 ratios.

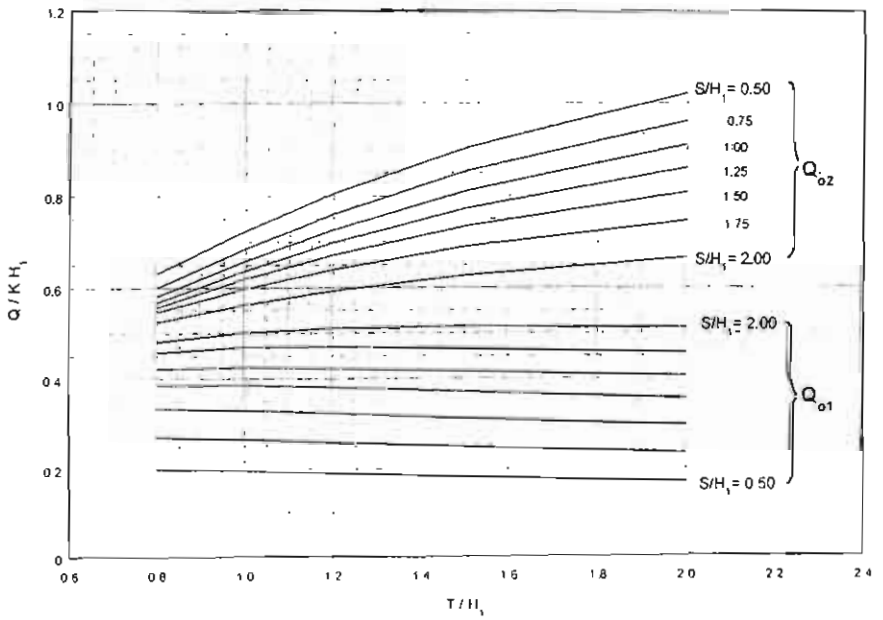

Fig.4 Outflow downstream the first and the second floors for all S/H_1 ratios.

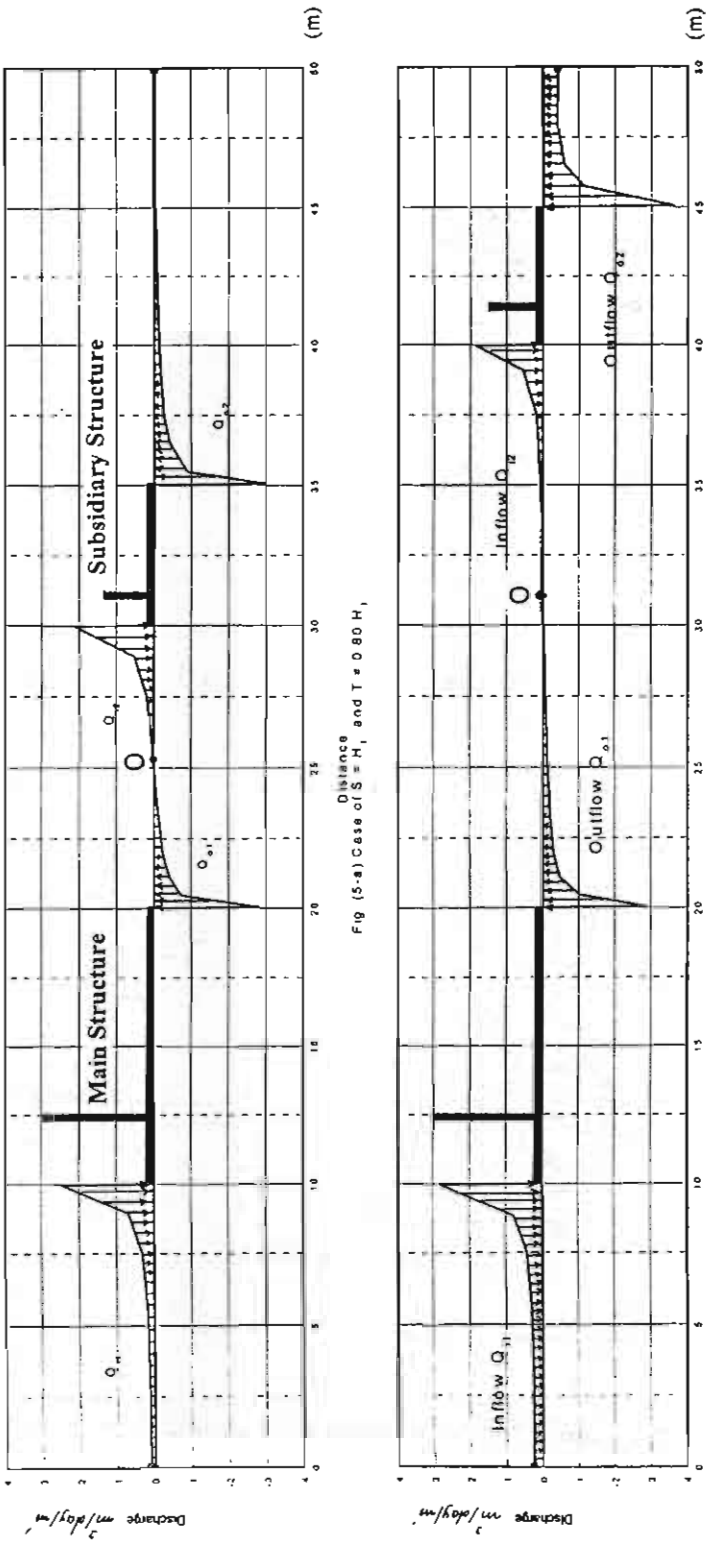

Fig (5-a) Case of S = H_1 and T = 0.80 H_1

Fig (5-b) Case of S = 2.0 H_1 and T = 2.0 H_1

Fig. (5) The Distribution of The Inflow - Outflow Seepage Discharge

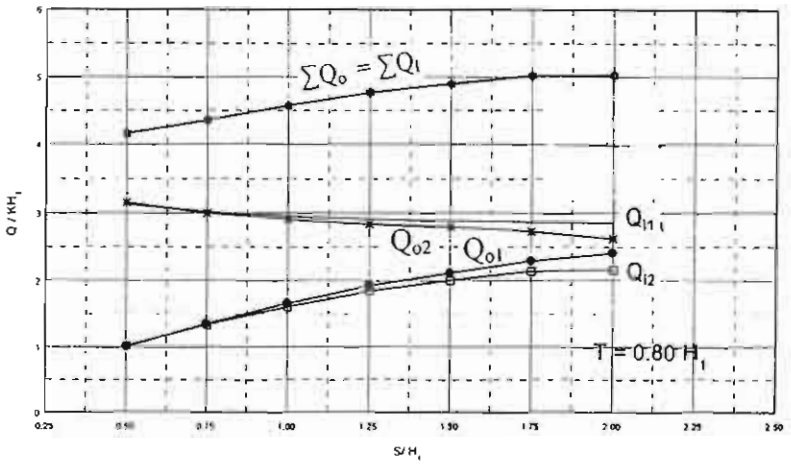

Fig. 6 Inflow- Outflow versus S/H_1 for $T/H_1 = 0.80$.

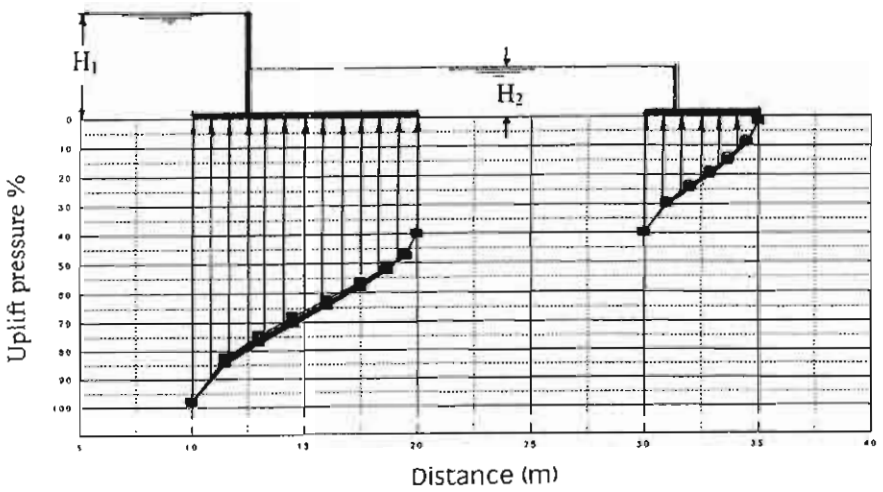

Fig. 7 Total uplift pressures on the first and second floors
For the considered cases of T/H_1, ($S=H_1$)

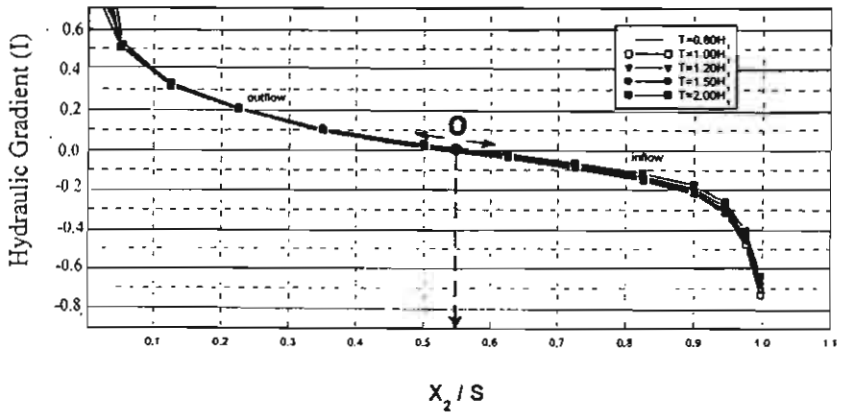

Fig. 8 Hydraulic gradient downstream the first floor ($S/H_1 = 2.0$)

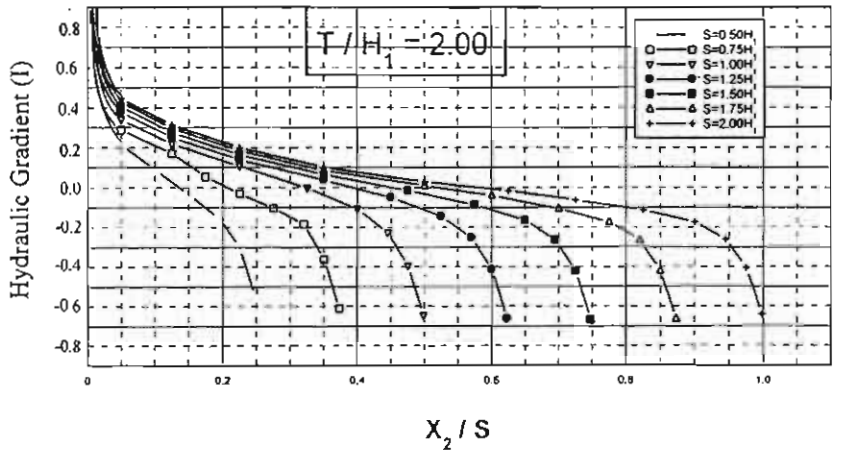

Fig. 9 Hydraulic gradient downstream the first floor ($T/H_1 = 2.0$)

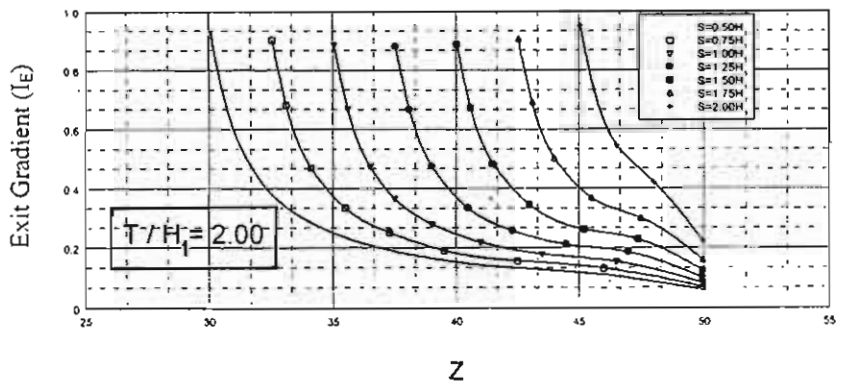

Fig. 10 Hydraulic gradient downstream the second floor ($T/H_1 = 2.0$)

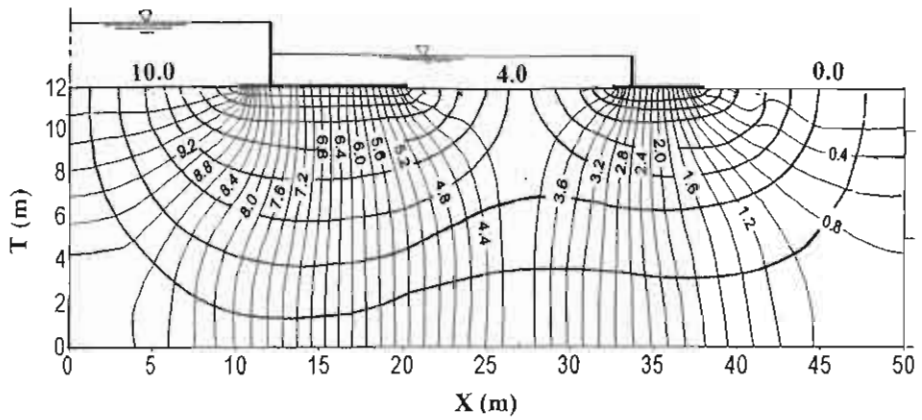

Flow-net for the case of T=1.2 H_1 and S = 1.25 H_1

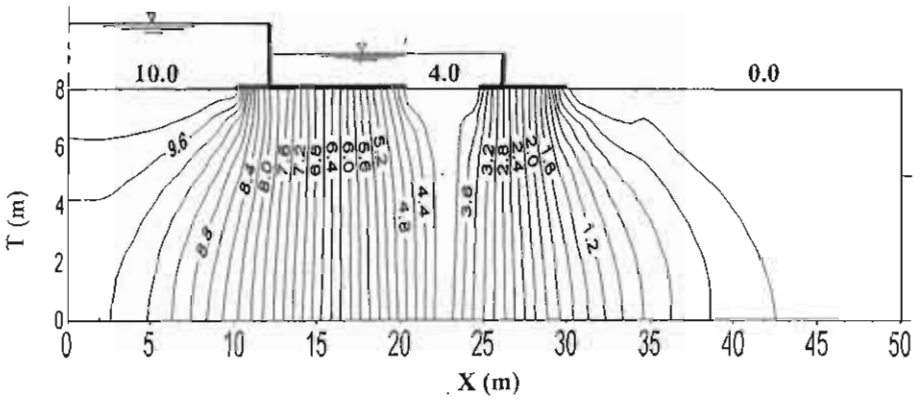

Equipotential lines for case of T = 0.8 H_1 and S= 0.5 H_1

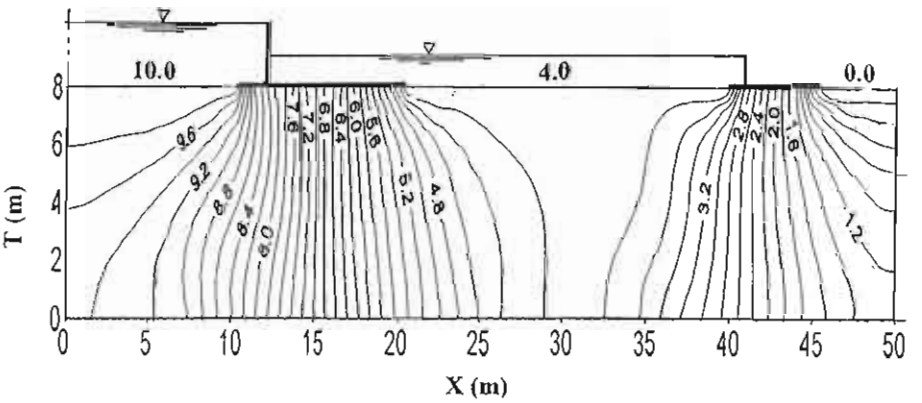

Equipotential lines for case of T = 0.8 H_1 and S= 2.0 H_1

Fig. 11 Flow net and equipotential lines for some cases